Robotics and Autonomous Systems 74 (2015) 340–350

Contents lists available at ScienceDirect

Robotics and Autonomous Systems

journal homepage: www.elsevier.com/locate/robot

Bio-inspired construction with mobile robots and compliant pockets

Touraj Soleymani [a,*], Vito Trianni [b], Michael Bonani [c], Francesco Mondada [d], Marco Dorigo [a]

[a] IRIDIA, Université Libre de Bruxelles, Ave. F. Roosevelt 50, CP 194/6, 1050 Brussels, Belgium
[b] ISTC, National Research Council, Rome, Italy
[c] Association Mobsya, Crissier, Switzerland
[d] LSRO, École Polytechnique Fédérale de Lausanne, Lausanne, Switzerland

HIGHLIGHTS

- Study of an autonomous construction system that uses compliant pockets.
- Development of a bio-inspired, stochastic control algorithm.
- Extension of the control algorithm to swarm construction.

ARTICLE INFO

Article history:
Available online 17 August 2015

Keywords:
Autonomous construction
Mobile robots
Compliant pockets
Stigmergy
Templates

ABSTRACT

In this paper, we develop an autonomous construction system in which self-contained ground robots build a protective barrier by means of compliant pockets. We present a stochastic control algorithm based on two biological mechanisms – stigmergy and templates – that takes advantage of compliant pockets for autonomous construction with single and multiple robots. The control algorithm guides the robot(s) to build the protective barrier without relying on a central planner, an external computer, or a motion capture system. We propose a statistical model to represent the structures built with the compliant pockets, and we provide a set of criteria for assessing the performance of the proposed system. To demonstrate the feasibility of the proposed system, real-robot and simulation experiments were carried out. The results show the viability of the proposed autonomous construction system.

1. Introduction

Robots could be the only viable alternative for construction and manipulation tasks in environments that are hazardous or inaccessible for humans [1], e.g., disaster areas, extraterrestrial surfaces, underground mines, or undersea. However, the employment of autonomous robots in these environments is still very challenging, and demands more research. Nature is one of the sources of inspiration that can help us in this regard. We can see, by observing nature, how simple agents employ adaptive and robust solutions to construct in dynamic and unstructured environments. Examples of such constructions include beaver dams, termite mounds, caddisfly cases, bee hives, social weaver nests, spider webs, and anthill structures. The construction of these structures is based on carefully evolved and well adapted rules. In particular, the usage of compliant materials along with special stochastic deposition rules can help coping with the uncertainties and the unpredictability of the environment. Our goal in this paper is to develop an autonomous construction system by taking inspiration from these biological examples.

We define *autonomous construction* a robotic activity in which one or many autonomous robots repeatedly *grasp, transport*, and *deposit* material in order to build a structure. In an autonomous construction system, we need to specify the task objective, which defines the form or function of the structure to be built; the building material of which the structure will be made; the autonomous robots that build the structure, in terms of their sensing, processing, and actuation capabilities; and the control algorithms that are implemented on the robots.

In this paper, we study an autonomous construction system whose task is to build a barrier exploiting filled bags as compliant material. Each robot in the system is a ground robot controlled by

* Corresponding author.
E-mail addresses: tsoleyma@ulb.ac.be (T. Soleymani), vito.trianni@istc.cnr.it (V. Trianni), michael.bonani@mobsya.org (M. Bonani), francesco.mondada@epfl.ch (F. Mondada), mdorigo@ulb.ac.be (M. Dorigo).

http://dx.doi.org/10.1016/j.robot.2015.07.018
0921-8890/

a reactive stochastic algorithm that exploits information already available in the environment. We describe the motivations for this study in terms of the above-mentioned aspects in the following.

1.1. Task objective

The task objective in this study is to build a protective barrier surrounding a generic dangerous area. The real-world applications that motivate our task objective – and therefore this study – include building radiation shields after nuclear disasters, lunar and Martian infrastructures like the one proposed in NASA's In-Situ Resource Utilization project [2], emergency shelters after earthquakes [3], and levees against tsunamis. The functional and performance requirements that are imposed by these applications include fast and simple realization, low cost, radiation exposure reduction, structure integrity, and impact resistance.

1.2. Building material

The building material must be chosen according to the task objective. In this work, we employ filled bags for building the protective barrier. The usage of this type of material, particularly in an autonomous construction system, is novel, and is coherent with some recent research. For example, Cal-Earth [3] proposes the use of sandbags for emergency shelters, and NASA [2,4,5] proposes the use of regolith bags for building lunar habitats.

Filled bags are built by enclosing some amorphous material into fabric pockets, so that they maintain a certain degree of deformability. As a consequence, filled bags (henceforth compliant pockets) have some of the properties of both rigid and amorphous materials, making them very appropriate for the autonomous construction of the aforementioned structures. In particular, they have the following features:

(i) They can conform to the shape of the environment in which they are placed. This property allows to construct on rough and uneven surfaces, and achieve packed structures. In addition, it makes quick deposition possible, because compliant pockets do not require edge alignment. Quick deposition can decrease the construction time.
(ii) They can fill voids in a structure. This property allows the robots to start building the structure simultaneously from different seeds as the different pieces of the structure can seamlessly join one another. In contrast, building structures with rigid parts requires to start from one seed [6]. Compliant pockets can remarkably improve the efficiency in parallel deposition.
(iii) They can be fabricated by exploiting in situ materials. Materials such as soil and sand on earth and regolith on the Moon, Mars, etc. are generally amorphous and cannot stay on their own. Compliant pockets are recognized as a simple, inexpensive, time-saving, and flexible approach for shaping these amorphous materials [2,3].

1.3. Autonomous robot

The robots must be equipped with the necessary sensors, processors, and actuators in order to be able to interact with the environment and manipulate the building material. In this study, each robot is completely self-contained, i.e., sensing, processing, and actuation are onboard. The robot is able to move and search for the building material in the environment. In addition, a manipulator with few degrees of freedom is sufficient for handling compliant pockets, thanks to the low precision required in their positioning and alignment.

1.4. Control algorithm

The control algorithm for autonomous construction should guide the robots to grasp the building material, transport it, and deposit it at the right place. Our control system uses two biological mechanisms – stigmergy and templates [7,8] – to achieve this goal:

(i) Stigmergy is the coordination of actions through modification of the environment by the agents. In stigmergy, the current state of the environment is the result of the previous building activity of the agents and it is used by the agents to guide their subsequent actions.
(ii) Templates are heterogeneities of the environment (e.g., a temperature gradient) that can be recognized by the agents and that can influence their behaviors. The final shape of the structure can be specified by the use of a template.

Adopting a control algorithm based on stigmergy and templates and exploiting the properties of the compliant pockets, the robots can compensate the uncertainties of the environment and organize the construction activities without the need of a blueprint or of any explicit representation of the structure to be built. Additionally, stigmergy and templates naturally lend themselves to cooperative construction in multi-robot systems, as discussed next.

1.5. Swarm construction

A swarm robotics system is an autonomous system in which multiple robots locally cooperate to accomplish a common task in a distributed fashion [9,10]. Swarm robotics systems can possess different functional properties. They can be *robust* against individual failures, *adaptive* against environment changes, *scalable* with respect to the swarm size, and *parallel* in work accomplishment. These properties make swarm robotics systems very appealing for applications such as autonomous construction.

The main challenge in swarm construction is how to design a distributed controller for the robots that allows them to cooperatively build a structure. Since interactions and communication between robots are local, coordination of activities between different robots to achieve the desired global structure is not trivial. In addition, interference between robots can degrade the performance of the system.

1.6. Contributions and outline

The contributions of our study are[1]: (i) the experimental investigation of the feasibility, merits, and performance of an autonomous construction system that uses compliant pockets as building material; (ii) the development of a bio-inspired, stochastic control algorithm that exploits the properties of compliant pockets for autonomous construction; (iii) the extension of the control algorithm to swarm construction and the analysis of the performance of such a system. The results presented in this paper are based on both simulation and real-world experiments.

The remainder of the paper is organized as follows. Related work is discussed in Section 2. The scenario definition, the specification of the building material and of the robots, and the architecture of the controller are provided in Section 3. The metrics used to evaluate the construction performance are presented in Section 4. Results of single-robot and multi-robot experiments are discussed in Sections 5 and 6, respectively. Finally, concluding remarks are made in Section 7.

[1] A preliminary version of the research presented in this paper was published in [11].

2. Literature survey

Autonomous construction has attracted much attention in the robotics community. In this brief survey, we limit ourselves to studies that develop an autonomous construction system by employing real robots.

2.1. Robotic construction systems

In a seminal work, Brooks et al. [12] proposed a system made of twenty robots, equipped with a behavior-based controller and a piling scoop for leveling soil on an artificial lunar surface. Melhuish et al. [13] used six simple robots to sort pucks along a line that served as a template. The structure was built by aligning pucks together, and was two-dimensional. Wawerla et al. [14] employed a single robot that used a behavior-based controller for building a two-dimensional structure made of cardboard blocks. These studies employ simple controllers, but are limited to aligning objects on a plane. We advance over these studies by taking advantage of compliant pockets for growing a structure in height.

Studies on three-dimensional construction employ planning-based controllers. Lindsey et al. [15] employed up to three quadrotors and a central planner to build framed structures out of beams and nodes. Willmann et al. [16] used four quadrotors to build a six meter tower with polystyrene modules. Wismer et al. [17] adopted a single ground robot to build a roofed structure with polystyrene blocks. In contrast to these studies, in our work the robot is completely self-contained, and does not rely on a central planner, an external computer, or a motion capture system.

Petersen et al. [18] developed a termite inspired construction system for building three-dimensional structures with a robot capable of moving on the structure made by specialized bricks, without using a motion capture system. In this work, a one-dimensional plan of the final structure, called "structpath", is evaluated off-line, and then it is used by the robot to build the structure. Recently, authors in [18] extended their work, and used three self-contained robots for building three-dimensional structures [6]. In these studies, a discrete model of the environment is used and deposition rules are deterministic while we use a continuous model and stochastic deposition rules.

2.2. Compliant and amorphous materials

Recent studies propose the usage of amorphous and compliant materials as a new avenue for autonomous construction in unstructured environments. Napp and Nagpal [19] developed a distributed, reactive algorithm for deposition of foam as amorphous material in order to build a navigable ramp for robots. They realized their system by using a remote controlled prototype robot and a scanning mechanism. Similar to [19], Revzen et al. [20] developed a modular robot capable of depositing foam in the environment, and Khoshnevis [21] proposed the "contour crafting" concept for building continuous structures by using a gantry system for deposition of amorphous material. Napp et al. [22] also studied the physical properties and the functional requirements of a number of compliant and amorphous materials for autonomous construction. In this paper, we develop an autonomous construction system with compliant pockets as building material, and we study the feasibility and performance of the system through experiments.

3. Autonomous construction system

In this section, we first introduce the scenario for the realization of our task objective. Then, we describe the compliant pockets and the ground robots used in our study. Finally, we discuss the architecture of our control algorithm in detail.

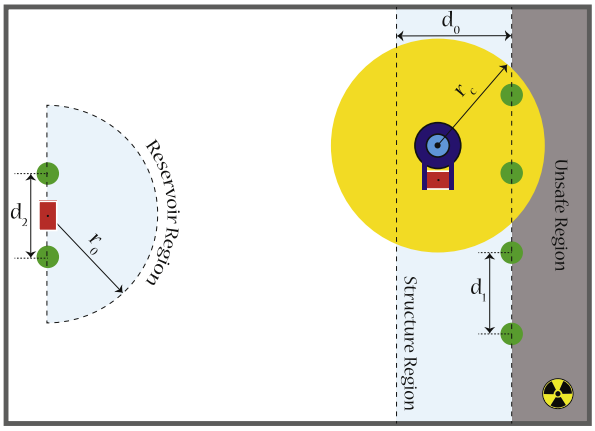

Fig. 1. Scheme of the arena. The unsafe, the structure, and the reservoir regions are specified (the sizes of the regions are approximate). The six green circles represent the landmarks. The line that traverses the four landmarks on the right side is the boundary. The robot, represented as a blue circle in the structure region, is carrying a pocket represented in red. The yellow circle around the robot shows the maximum range of the robot's omni-directional camera. Another pocket is placed in the reservoir region between the two landmarks. The values of d_0, r_c, d_1, r_0, and d_2 used in the experiment are given in the Appendix. (For interpretation of the references to color in this figure legend, the reader is referred to the web version of this article.)

3.1. Construction task: building a protective barrier

The scenario is schematically depicted in Fig. 1. The task consists in building a barrier with a specified width and length by stacking n_{tot} pockets. The barrier is intended to provide a "safe" region in front of an "unsafe" region in the arena (see Fig. 1).

The arena is a closed rectangle. A number of landmarks, situated in the arena, serve as a template and specify the position and shape of the barrier. Note that the global position of the landmarks is not available to the robots. The safe and unsafe regions are separated by an imaginary frontier called *boundary*. The boundary consists of lines that connect the landmarks of the template to one another. We refer to these lines as *boundary lines*, and their length is denoted by d_1. Depending on the position of the landmarks, the boundary can have different shapes. In our case, it is linear. There might be one or more locations where pockets are available to be grasped. Each location is specified by an additional pair of landmarks.

We refer to the abstract region in which the deposition activity of the robots takes place as *structure region*. This region is defined in a way that if a robot is there, it can see at least two landmarks. The width d_0 of the structure region is therefore a function of the inter-landmark distance d_1 and the range of the robot's omni-directional camera r_c. We call the abstract region in which the grasping activity of the robots takes place *reservoir region*. This region is defined by a semicircle of radius r_0, and if a robot is there, it can see both pocket and two landmarks. Therefore, r_0 is a function of the distance between the two landmarks d_2 and of the camera range r_c. The location of the pocket in the reservoir region is also referred to as *grasping point*. Whenever a pocket is picked up by a robot, a new one is added manually at the grasping point, with its longitudinal axis aligned with the two landmarks. The robots commute between the reservoir and the structure regions. They grasp pockets in the reservoir region, and deposit them in the structure region to build the protective barrier.

3.2. Building material: compliant pockets

The adopted pockets are passive, simple, and inexpensive. They were built by hand in short time and without high precision. A sample of these pockets is shown in Fig. 2. Each pocket is composed

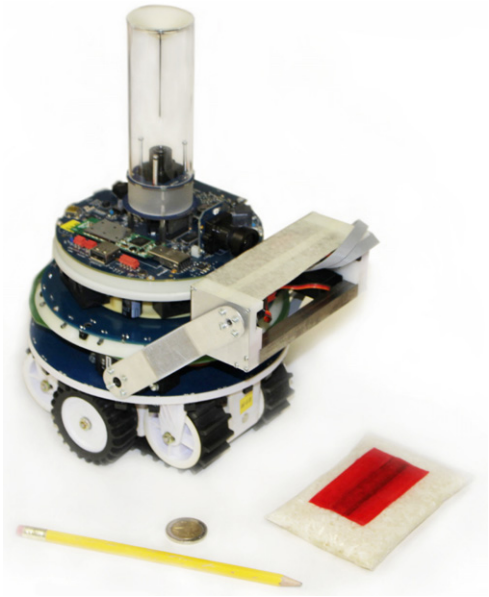

Fig. 2. A marXbot robot with its manipulator, and, on its right, a compliant pocket.

of a plastic bag filled with dry rice grains, in a manner that allows its shape to change to some extent under force exertion. A stripe of ferromagnetic metal is attached along the longitudinal axis of each pocket and is used to facilitate grasping by the robot, as described below. A red tape maintains this metal strip in position, and also makes the pocket visually recognizable by the robot's camera. Each pocket weighs approximately 100 g, is 12 cm in length, 7 cm in width, and 1.5 cm in height. The size and weight of the pockets are chosen in a way that is compatible with the specifications of the robot's manipulator.

3.3. Autonomous robot: the marXbots

We employ marXbots [23], miniature, modular, all-terrain experimentation robots developed within the Swarmanoid project [24] (see Fig. 2). The robot is 17 cm in diameter and 29 cm in height.

The robots can sense the environment mainly through the omni-directional camera, from which colored blobs are extracted that allow discriminating between landmarks, pockets and other robots, as well as calculating the approximate distance and bearing. Proximity sensors are used for the detection of pockets and obstacles. Motor encoders provide the necessary information for odometric navigation. The robot moves using a differential drive system that is a combination of tracks and wheels—referred to as *treels*. It can grasp pockets by means of a simple two degrees-of-freedom manipulator [25]. The manipulator can lay on the ground in order to detect a pocket, and can rise to pick up a pocket. At the base of the manipulator, there are 6 infrared proximity sensors and a magnet that can be activated or deactivated to grasp or drop pockets.

Notice that the use of metal and magnet in the design of the pockets and manipulator is just one possible solution; any other design that allows the robot to reliably grasp and drop pockets would be a feasible choice.

3.4. Control algorithm: using stigmergy and templates

We design a finite-state controller with three states devoted to exploring the environment, loading, and unloading compliant pockets. We first develop the controller for the single-robot system, and then extend it for the multi-robot system.

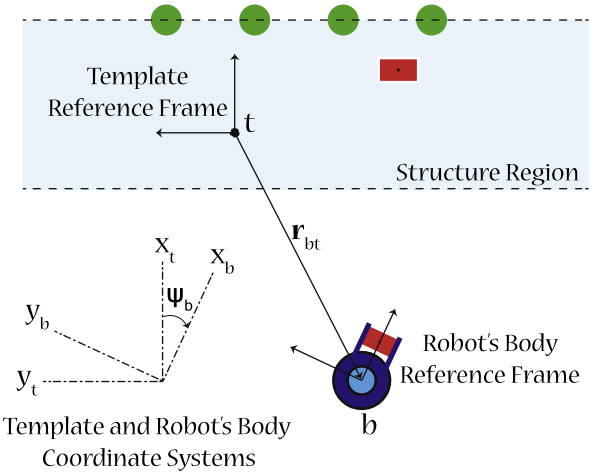

Fig. 3. Template reference frame and template coordinate system. The robot exploits the template reference frame and template coordinate system when it is outside the structure and the reservoir regions.

Let us refer to a complete set of activities that a robot needs to perform from grasping to depositing a pocket as an iteration. In each iteration, the relative position of the robot is computed by the odometric navigation equations which allow the robot to commute between reservoir and structure regions, as discussed below. Within these regions, the relative location of landmarks and pockets is obtained through the visual image processing following a dedicated calibration procedure [26]. In order to make odometric and visual navigations possible, we need to utilize appropriate reference frames and coordinate systems.

3.4.1. Odometric navigation

We introduce the *template reference frame*, a flexible reference frame with origin (i.e., reference point) any arbitrary point within the structure region, and with the positive direction of its x-axis perpendicular and pointing to a boundary line. The robot exploits the template reference frame in its odometric navigation to move between the structure and the reservoir region. The template reference frame is not fixed, but rather it is modified by the robot itself at each iteration after the deposition of a pocket. Preliminary tests determined that the accumulated error during odometric navigation between reservoir and structure region is compatible with the completion of an iteration. At the end of each iteration, the template reference frame is reinitialized and the accumulated error is canceled.

The location of the robot b with respect to the template reference point t expressed in the template coordinate system $|t$ is denoted by $\boldsymbol{r}_{bt}^{|t} = [x_{bt}^{|t}, y_{bt}^{|t}]^T$, and its relative angle is ψ_b (see Fig. 3). Both are updated by solving the odometric navigation equations. The grasping point g is also expressed with respect to the template reference point t and in the template coordinate system $|t$, and is denoted by $\boldsymbol{r}_{gt}^{|t} = [x_{gt}^{|t}, y_{gt}^{|t}]^T$. In order to execute the control commands in odometric navigation, the robot employs the transformation matrix between its body coordinate system $|b$ and the template coordinate system $|t$, denoted by $\boldsymbol{C}^{|bt}(\psi_b)$.

3.4.2. Visual navigation

When the robot is in the structure (or reservoir) region, the projection of the robot's location on the closest boundary line (or the line that connects the two landmarks in the reservoir) is a point which is denoted by p. We define the *projection coordinate system* with the x-axis in the direction of the vector pointing from the robot b to the point p (see Fig. 4). The robot employs the projection coordinate system $|p$ in its visual navigation to

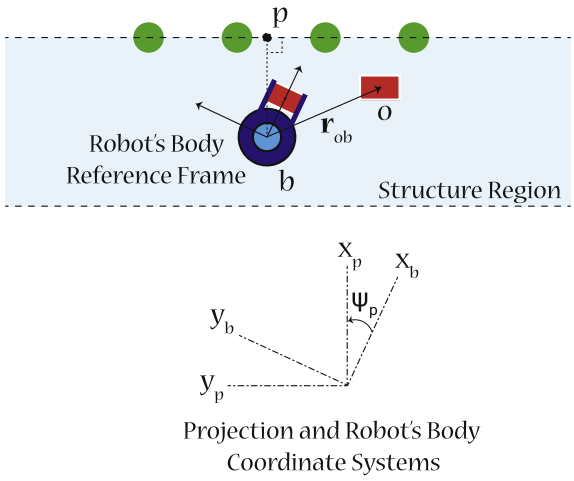

Fig. 4. Projection coordinate system. The robot exploits the projection coordinate system when it is inside the structure region.

navigate within the structure region (with an arbitrary boundary's shape) and within the reservoir region. The transformation matrix between the robot's body coordinate system $|b$ and the projection coordinate system $|p$ is denoted by $\boldsymbol{C}^{|pb}(\psi_p)$, where ψ_p is the relative angle of the point p in the body coordinate system, and is obtained through image processing.

3.4.3. Single-robot controller

In the following, we describe the three states of the control algorithm, and transitions between them (see Fig. 5).

Explore state. The explore state allows the robot to acquire information about the structure and reservoir regions. The robot searches in the arena, while avoiding collisions with walls, landmarks, and pockets. When the robot enters the structure region, it constructs the template reference frame, and initializes it. When it enters the reservoir region, it saves the coordinates of the grasping point in the template coordinate system. If the reservoir region is detected earlier than the structure region, the robot updates the coordinates of the grasping point after entering the structure region. Once both structure and reservoir regions are detected (i.e., the template reference frame and the grasping point are initialized), the load state is activated.

The explore state is also considered as a recovery state. In particular, if the robot fails reaching the desired region while in the load or unload states, it recovers to the explore state.

Load state. In the load state, the robot uses odometric navigation to reach the reservoir region. When the robot enters this region, it uses the vision sensor to detect the two landmarks and the pocket. For the alignment of the manipulator with the pocket, the approach trajectory should roughly be normal to the pocket's longitudinal axis. The robot first moves toward a specified point in front of the pocket. It lowers the manipulator, and moves forward until it detects the pocket through the proximity sensors of the manipulator. Then, it raises the manipulator to the top of the pocket, activates the magnet, and picks up the pocket. At this time, the robot saves the coordinates of the current location as the coordinates of the grasping point, and the unload state is activated.

Unload state. In the unload state, the robot uses odometric navigation in order to reach the structure region. When the robot enters this region, the controller should choose an appropriate deposition point and guide the robot toward it.

In construction with pockets, the orientation of the deposition point is not required thanks to the pockets' deformability, and its height is specified directly by the structure itself through

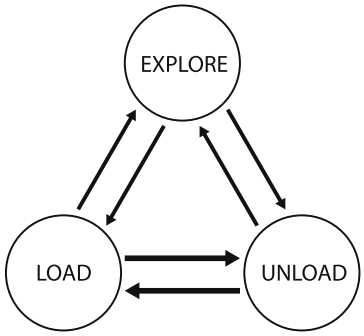

Fig. 5. Three states of the controller (i.e., explore, load, and unload) with the transitions between them. The thicker arrows between the load and unload states indicate the main loop exploited during construction activities.

the stacking process. Therefore, the deposition point d can be specified using only two coordinates (i.e., $\boldsymbol{r}_{dt}^{|t} = [x_{dt}^{|t},\ y_{dt}^{|t}]^T$ with respect to the template reference point t and expressed in the template coordinate system $|t$) instead of six coordinates in the three dimensional space. In the following, we explain in detail how the controller chooses the two coordinates of the deposition point by making decisions based on two complementary stochastic rules, one for the y and the other for the x coordinate.

Assuming that the robot is in the structure region, the vision sensor can detect a part of the template and of the structure. First, the robot randomly chooses a direction (right or left). Then, it moves along a path parallel to the boundary (see Fig. 6). If the robot reaches one of the ends of the boundary, it turns around and continues moving in the opposite direction.

Suppose n pockets have been deposited at time t, and let $\boldsymbol{r}_{o_ib}^{|b}$ denote the location of the center of mass of the ith pocket o_i with respect to the robot b expressed in the robot's body coordinate system $|b$. The set of visible pockets $\mathcal{N}_v$ is defined as

$$\mathcal{N}_v = \{j \in \{1, \ldots, n\} : \|\boldsymbol{r}_{o_jb}^{|b}\| \leq r_c\} \tag{1}$$

where $\boldsymbol{r}_{o_ib}^{|b}$ for all $i \in \mathcal{N}_v$ is given by the camera for the detected pockets. One can express the location of a visible pocket o_i with respect to the robot b in the projection coordinate system $|p$ by the transformation $\boldsymbol{r}_{o_ib}^{|p} = \boldsymbol{C}^{|pb}\boldsymbol{r}_{o_ib}^{|b}$ with the components $\boldsymbol{r}_{o_ib}^{|p} = [x_{o_ib},\ y_{o_ib}]^T$. Note that stacked pockets can be detected as long as they are not completely covered by other pockets.

We define the set of influential pockets $\mathcal{N}_f$ based on the y-component of the locations of the visible pockets:

$$\mathcal{N}_f(\delta) = \{j \in \mathcal{N}_v : -\delta \leq y_{o_jb} \leq \delta\} \tag{2}$$

where δ is a parameter.

Stochastic axial rule. At each control step, the probability that the robot chooses $y_{bt}^{|t}$ along the length of the structure for the deposition is:

$$P\big(y_{dt}^{|t} = y_{bt}^{|t};\ |\mathcal{N}_f(\delta_1)|\big) = \frac{k_1}{1 + \alpha^2|\mathcal{N}_f(\delta_1)|^2} \tag{3}$$

where $|\mathcal{N}_f|$ denotes the size of the set $\mathcal{N}_f$, k_1 is a scaling factor, and δ_1 and α are constant. Eq. (3) implies that if the number of pockets in an area is low, the probability of depositing the carried pocket is high and *vice versa*. Notice that the axial rule is based on negative feedback. It allows the robot to explore along the length of the structure and to fill voids. Once the robot has made the decision, it turns and moves toward the structure.

Stochastic lateral rule. At each control step, the probability that the robot selects $x_{bt}^{|t}$ along the width of the structure for the deposition is:

$$P\big(x_{dt}^{|t} = x_{bt}^{|t};\ \mu(\delta_2)\big) = k_2 \exp\Big(-\frac{\mu^2(\delta_2)}{\sigma^2}\Big) \tag{4}$$

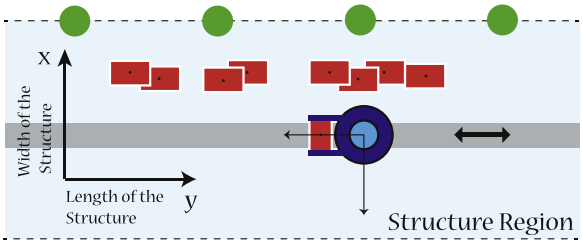

Fig. 6. A robot in the structure region moving on a path along the structure. Both directions are admissible on the path.

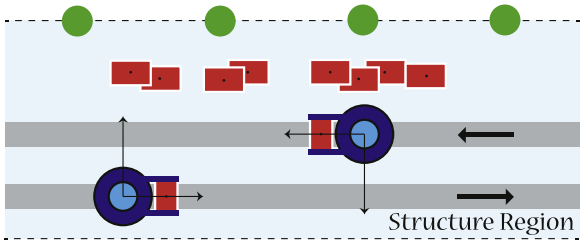

Fig. 7. Two robots in the structure region moving on the main path (upper one) and the auxiliary path (lower one). The paths have uni-directional traffic. Only the robot on the main path is allowed to deposit the pocket.

where k_2 is a scaling factor, δ_2 and σ are constant, and μ is defined as

$$\mu(\delta_2) = \frac{1}{|\mathcal{N}_f(\delta_2)|} \sum_{j \in \mathcal{N}_f(\delta_2)} x_{o_j b} - x_0 \tag{5}$$

where x_0 is the distance between the center of the manipulator and the center of the robot. Eq. (4) implies that the robot deposits the carried pocket with higher probability where the density of pockets along the width of the structure is higher. Note that the lateral rule is based on positive feedback and maximizes the compactness of the structure along its width.

In summary, the axial and lateral rules are designed based on stigmergy and on a template. The template forms the boundary line, and stigmergy affects the decision making.

When the deposition point is reached, the robot deactivates the magnet of the manipulator, and lets the pocket drop thanks to the gravitational force. The robot then reinitializes the template reference frame based on its current state, and updates the coordinates of the grasping point. This eliminates the accumulated error in the odometric navigation from the previous iteration. At this stage, the current iteration finishes, and the next iteration starts with the load state.

3.4.4. Multi-robot controller

In order to use the designed controller for swarm construction some modification are necessary. These are described in the following.

Distributed frame. We recall that the template reference frame is a reference frame defined independently for each robot. This frame plays an important role in decentralization of the control algorithm as it relaxes the need of having a global reference frame for the navigation of the robots. The template reference frame is initialized by each robot in the explore state, and it is then updated at the end of each iteration in the unload state. Although the template reference frame is constructed, initialized, and updated independently by each robot, it organizes the construction activities of the robots in the swarm construction.

Interference resolution rules. As the robots move to carry out their activities, their trajectories might intersect with one another. We develop interference resolution rules that allow each robot to move toward its target while avoiding collisions with other robots in a distributed fashion.

If it is in the explore state, or if it is commuting between reservoir and structure regions, the robot changes its velocity direction away from the collision course. If it is in the reservoir region, the robot waits without moving until its closest reservoir becomes available. Interference resolution in the structure region is more complex. Notice that in our autonomous construction system, robots build the structure using local decisions. Therefore, the robots have to locally observe the structure by moving along it. In the controller designed for a single robot, we assumed that the robot uses a path in the vicinity of the structure. However, as the number of robots increases, a more efficient way for the movement of the robots in this critical region is needed.

We propose to use two paths that are parallel to the boundary. We call the closer path to the boundary the main path with leftward traffic direction, and we call the farther one the auxiliary path with rightward traffic direction (see Fig. 7). A robot always uses the auxiliary path when it enters the structure region. Then, it checks for any robot on its left side. If there is no robot, it turns and enters the main path. Otherwise, it continues until its left side becomes free. We assume that deposition is only allowed when the robot is in the main path. Once the robot deposits the pocket, it moves in the main path until its left side becomes free. Then, it goes toward the reservoir region. Note that if a robot stops in a path, for example for dropping a pocket, the robots close behind it also stop temporarily.

Stochastic directional rule. Based on the interference resolution rule, the robots can deposit pockets when they are in the main path, and within the main path they can only move leftward. As a consequence, the probability of visiting the left side of the structure is higher than for the right side, hence resulting in an asymmetry in the exploration. To resolve this asymmetry, we use a stochastic rule that allows the robots to enter the auxiliary path from the main path and *vice versa*. Let $s = \{L, R\}$ denote a state representing whether the robot is in the main path or in the auxiliary path, respectively. The probability that the robot changes this state is defined as

$$P\big(s = L|s = R\big) = P\big(s = R|s = L\big) = \nu \tag{6}$$

where $\nu \in [0, 1]$ is a parameter. The mean traveled distance along a path is a function of ν. The directional rule results in a uniform exploration of the structure in the main path. Note that when a robot reaches the ends of the boundary, it is forced to change the state s.

4. Metrics

In this section, we introduce a statistical model for the structures built with compliant pockets. Then, we propose a set of criteria for assessing the quality of the built structures.

4.1. Statistical model of the structure

To study the quality of the choices made about the deposition points ($x_{dt}^{|t}$ and $y_{dt}^{|t}$), we analyze the effect of these decisions on the resulting structure after a finite number of depositions.

One way for describing the structure is to use height functions as suggested for amorphous materials in [19]. The height function $h(\mathbf{x}) : \mathbb{R}^d \rightarrow \mathbb{R}_{\geq 0}$ can be defined as the height of the exterior surface of the structure over the one- or two-dimensional construction domain ($d = 1, 2$).

A more appropriate way for representing the constructed structure with compliant pockets is to use the distribution of

pockets in space. This is because pockets are discrete and countable objects. Additionally, there is some inherent uncertainty in the deposition that can be grasped by means of a statistical model. We propose to use *kernel density estimation* to obtain a model for structures with pockets. Kernel density estimation is a non-parametric approach for estimating the density function of a finite set of data samples [27]. Let $\mathbf{x} \in \mathbb{R}^d$ denote the d-dimensional location of a pocket in an arbitrary coordinate system. The multivariate kernel density function $f(\mathbf{x}) : \mathbb{R}^d \rightarrow \mathbb{R}_{\geq 0}$ of a structure with compliant pockets after n depositions is defined as

$$f(\mathbf{x}) = \frac{1}{n}\sum_{i=1}^{n} K_H(\mathbf{x} - \mathbf{x}_i) \tag{7}$$

where $K_H(\mathbf{x})$ is

$$K_H(\mathbf{x}) = |H|^{-1/2}\, K(H^{-1/2}\mathbf{x}) \tag{8}$$

where H is a symmetric positive-definite $d \times d$ matrix called the bandwidth matrix and $K(\mathbf{x})$ is the kernel function. The kernel in our study is a normal density function:

$$K(\mathbf{x}) = \frac{1}{(2\pi)^{d/2}} \exp\left(-\frac{1}{2}\mathbf{x}^T\mathbf{x}\right). \tag{9}$$

In order to evaluate the kernel density function for the whole structure, we require only the location of the pockets' center of mass. We associate a kernel to each pocket, and we model the accumulation of pockets by the summation of the corresponding kernels.

A density function can account for the distribution of deposition points resulting from probabilistic local decisions. Furthermore, it takes into account the uncertainties in the shape and the final location of compliant pockets.

4.2. Performance criteria

Assume that we have the two-dimensional locations of the pockets $[x_i,\ y_i]^T$ for all $i \in \{1, \ldots, n\}$ after n depositions. To provide a quantitative evaluation of the proposed system, we define four criteria: uniformity error, integrity deviation, maximum gap, and deposition rate.

Uniformity error. It measures the difference between the pockets' distribution over the y-axis, resulting from a one-dimensional KDE estimation (7), and a uniform reference distribution along the length of the structure. The uniformity error after n depositions is defined as

$$e_y = \frac{1}{2A}\int_a^b \left|f(y) - f_0(y)\right| dy \tag{10}$$

where a and b are the extremities of the structure (we truncate the domain at the center of the leftmost and rightmost pockets), $f_0(y)$ is the uniform reference distribution, and $A \approx 1$ is the integral of the kernel density function over the domain. The factor 2 in the denominator is for normalization resulting in a theoretical maximum uniformity error of 1. By construction, the following property holds in the interval $[a, b]$:

$$\int_a^b f_0(y) = \int_a^b f(y) = A. \tag{11}$$

Low values of e_y correspond to more uniform structures.

Integrity deviation. It represents the compactness of the structure. It is defined as the standard deviation of the pockets' distribution along the width of the structure after n depositions

$$\sigma_x = \sqrt{\frac{1}{n-1}\sum_{i=1}^{n}(x_i - \bar{x})^2} \tag{12}$$

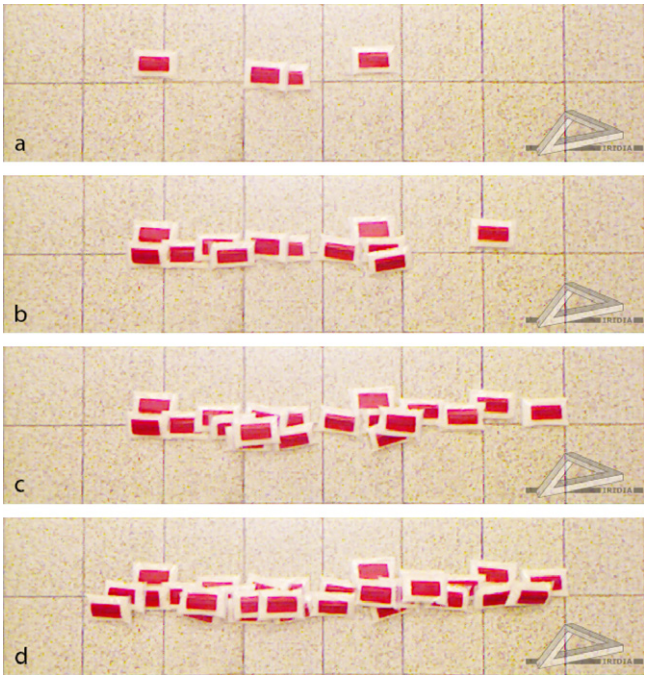

Fig. 8. Snapshots of the structure at different time steps. From top to down: (a) $t = 261$ s, $n = 4$, (b) $t = 869$ s, $n = 12$, (c) $t = 1425$ s, $n = 19$, (d) $t = 2366$ s, $n = 30$.

where $\bar{x}$ is the mean of the x-component of the pockets' locations. Low values of σ_x indicate high coherence of the structure along its width.

Maximum gap. It is defined as the maximum axial distance between two adjacent pockets after n depositions

$$g_{\max} = \max_{i,j\in\{1,\ldots,n\}, i\neq j}\{y_j - y_i\} \tag{13}$$

$$\text{s.t.}\ \ y_j > y_i, \quad \forall k \in \{1, \ldots, n\}, y_k > y_i \rightarrow y_j \leq y_k.$$

Low values of $g_{\max}$ are desirable.

Deposition rate. It is the average number of deposited pockets per unit time (minute) that is

$$q_{avg} = n/t \tag{14}$$

where t is the time required for constructing a structure with n pockets.

5. Single-robot experiments

The first set of experiments is targeted to evaluate the effectiveness of the proposed solution using a single physical robot. The setup of the experiments is as follows. The task consists in building a barrier approximately 120 cm long and 10 cm wide by stacking 30 pockets. The arena size is a 240 cm × 170 cm. Four landmarks specify the template, and only one reservoir is considered. The distance between the reservoir region and structure region is of approximately 190 cm. In order to track the growth of the structure, we mount a Microsoft Kinect® on top of the structure region that captures the RGB and depth images of the structure at different time steps.

Twenty trials were carried out (the parameters used in our experiments are reported in the Appendix). We provide the detailed

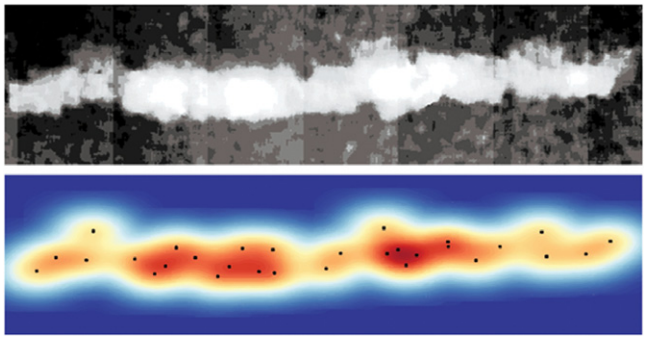

Fig. 9. Top: depth map of the final structure for the selected trial. Bottom: The corresponding bivariate kernel density function.

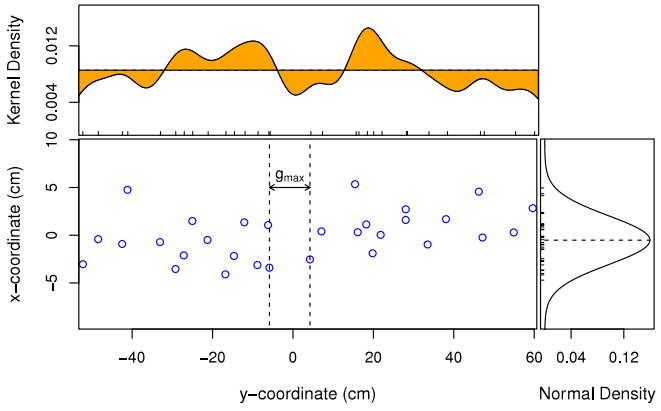

Fig. 10. Bottom left: two-dimensional distribution of pockets in the final structure for the selected trial. The maximum gap $g_{\max}$ is shown in the plot. Top: univariate kernel density function along the length of the structure compared to the corresponding uniform density function. The uniform deviation is calculated based on the area of the colored region. Bottom right: normal density function fitted to the distribution of pockets along the width of the structure. The integrity deviation is the estimated standard deviation of this function. (For interpretation of the references to color in this figure legend, the reader is referred to the web version of this article.)

results of one selected trial.[2] Fig. 8 illustrates the construction process through some snapshots of the structure at different time steps. After each deposition, the depth image of the structure was captured using the Kinect. The depth map representing the height function is shown in Fig. 9 for the final structure. Through image processing, by comparing each two consecutive depth images of the growing structure, the last deposited pocket was recognized, and its two-dimensional location in a coordinate system was extracted. Therefore, the two-dimensional locations of the pockets $[x_i,\ y_i]^T$ for all $i \in \{1, \ldots, n\}$ are available for our analysis. We computed the bivariate kernel density function for the final structure by choosing a diagonal bandwidth matrix with elements h_1 and h_2 for the x- and y-directions, respectively. Fig. 9 depicts the depth map diagram of the bivariate kernel density function. We observe a close correspondence between the height function and the kernel density function, which supports the choice of the latter as a model for the structure.

The performance criteria were evaluated for all trials. In the specific case of the selected trial (see Fig. 10), their values for the final structure are: $e_y = 0.13$, $\sigma_x = 2.50$ cm, $g_{\max} = 10.07$ cm, and $q_{avg} = 0.76$ min^{-1}.

[2] The video of the real-robot experiment is available at: http://iridia.ulb.ac.be/supp/IridiaSupp2015-003.

Fig. 11 reports the performance of the autonomous construction system based on the four criteria for 20 trials. We discuss only the medians of criteria as the dispersions are acceptably small. The median of the uniformity error is $\tilde{e}_y = 0.13$, which shows 13% deviation from the uniform distribution. This indicates that the built structures are roughly uniform obtaining an approximately constant height. The median of the integrity deviation is $\tilde{\sigma}_x = 2.44$ cm. It suggests that pockets are placed in the range ± 7.32 cm, that is $\pm 3 \times \tilde{\sigma}_x$, around the average. This range is twice the width of a pocket, meaning that the built structures are very coherent, integrated, and packed. The median of the maximum gap is $\tilde{g}_{\max} = 10.48$ cm. It is less than the axial distance between two pockets without overlapping (the length of each pocket is 12 cm). It indicates that the robot filled most of the voids in the structure. Finally, the median of deposition rate is $\tilde{q}_{avg} = 0.72$ min^{-1}. It means that each iteration took about 83 s on average. Considering the average speed of the robots ($\approx$10 cm/s), the distance between the reservoir and the structure regions, and the average time for grasping one pocket ($\approx$15 s), the robot spends on average approximately 30 s for each deposition.

Overall, by analyzing the structures built in all trials using the above metrics, we can conclude that our autonomous construction system is successful in building a uniform and integrated protective barrier in a reasonable time. This is thanks to the exploitation of the properties of compliant pockets, which allowed to employ simple deposition rules that resulted in uniform, integrated, void-free structures.

6. Multi-robot experiments

In this section, we study swarm construction through simulation experiments. The reason for resorting to a simulated model is that we can readily study and assess the performance of the autonomous construction system with an arbitrary size. In the following, we first discuss the validation of the simulated model. Then, we present the results of multi-robot experiments to demonstrate swarm construction. Finally, we study the effects of group size on the system performance.

6.1. Validation of the simulation

We adopt ARGoS, a fast high-fidelity multi-robot simulator [28]. The robot MarXbot has already been simulated, tested, and verified in this simulator with all of its main subsystems in previous studies [29–32]. For the purpose of this study, in addition we require an appropriate simulated model for compliant pockets that can match functional properties of the real pockets.

The interaction of the robots with the pockets is mainly based on visual perception. In the simulator, the omni-directional camera is modeled geometrically. Thus, the distance and relative angle of the center of mass of each object (acquired through image processing in reality), are available by geometric calculations. We corrupt these outputs of the camera with some noise to make the model more realistic. In addition, we need to consider the occlusion caused by the stacked pockets. To this end, we employ a simple model that associates to each pocket a value, i.e., the percentage of occlusion. This value decreases as a function of the pocket's area occluded by other pockets stacked on top, and can be calculated knowing the deposition points of the stacked pockets. We assume that a pocket is not visible anymore by the robot if the value is less than a specific threshold.

We ran simulations with a single robot with the same setup introduced earlier, and compared the results with the real-robot experiments in terms of the four performance criteria (see Fig. 11). Based on this investigation, the simulation was validated, and the appropriate modeling parameters were obtained. The modeling parameters remain fixed in the multi-robot experiments.

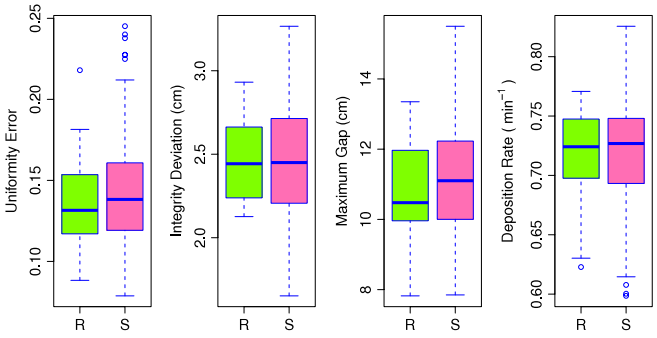

Fig. 11. Box plot diagram of the uniformity error, integrity deviation, maximum gap, and deposition rate for the real-robot experiments (R) and the simulation experiments (S) with 20 and 200 trials, respectively.

6.2. Scalability analysis

An important issue when considering a multi-robot system is the presence of physical interferences between the robots. Interferences decrease the performance of each robot, and can therefore hinder the system scalability. We study the scalability of our autonomous construction system by incrementally increasing the size of the group.

We first modify the size and setup of the arena so as to accommodate more robots. The size is changed to 400 cm × 600 cm. As before, the unsafe region is in one side of the arena and the reservoir is in the other side. The boundary is now made of 20 landmarks that form a 350 cm straight line. We increase the number of reservoirs to five. The distance between a reservoir region and the structure region is of approximately 330 cm. In this setup, 112 pockets are to be deposited in the structure region.

For scalability analysis, we ran simulation experiments in the new setup for different group sizes ranging from 1 to 8 robots.[3] For each group size, 200 simulation trials were carried out. Fig. 12 illustrates the mean and standard deviation of the four criteria versus the group sizes. The quality of the built structure in terms of uniformity error, integrity deviation, and maximum gap stays almost constant. This means that, despite the presence of interferences, the final structure is similar to the one built by a single robot. However, the deposition rate increases rapidly. This increment in the construction speed shows the advantage of parallelism of the robots in the accomplishment of the common task.

As said earlier, interferences between robots degrade the performance of each robot in the multi-robot system with respect to the single robot system. Differently, in an ideal condition without interferences, the increment in the size of the group does not affect the performance of each robot, and therefore the deposition rate in the multi-robot system can be obtained by multiplying the deposition rate in the single-robot system by the size of the group. Let $q^*_{avg}(m)$ denote the deposition rate in the ideal system with m robots, and $q_{avg}(m)$ denote the deposition rate in the implemented system with m robots. Then, the following relation holds:

$$q^*_{avg}(m) = mq_{avg}(1). \tag{15}$$

Note that $q^*_{avg}(1) = q_{avg}(1)$. Fig. 13 illustrates the deposition rates for the ideal and implemented systems versus the size of the group. The deviation from the straight line shows the degradation due to inferences.

[3] The video of the simulation experiment with 5 robots is available at: http://iridia.ulb.ac.be/supp/IridiaSupp2015-003.

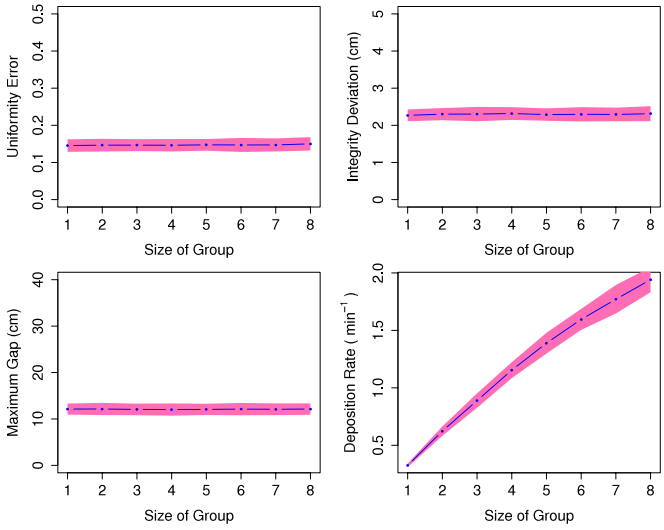

Fig. 12. The effect of the size of the group on the performance criteria, represented by the mean and standard deviation of 200 simulation trials.

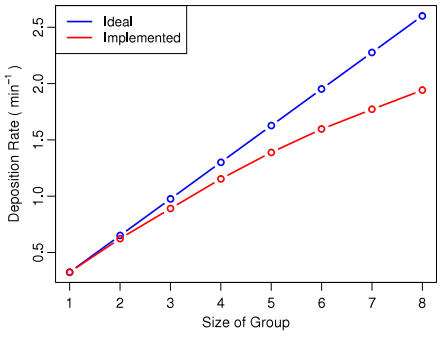

Fig. 13. Deposition rate versus the size of the group for the ideal system and the implemented system.

7. Conclusion

In this work, we developed an autonomous construction system for building structures out of compliant pockets deposited by multiple autonomous robots. We developed a control algorithm that exploits two biological mechanisms, namely stigmergy and templates. Thanks to these mechanisms and to the properties inherent to compliant pockets, we were able to deploy a system that allows robots to build a uniform, integrated, and void-free barrier.

It is worth noting the holistic approach taken in this work: the different components of the autonomous construction system are intimately related to each other. First of all, the task objective specifies the structure in terms of its requested form and function—in our case providing a protective barrier between a safe and an unsafe region. This justifies the usage of templates as a way to determine the structure shape, given that the structure must match the environmental features. The usage of compliant pockets enables simple and stochastic deposition rules, making it possible to fully exploit stigmergy as a coordination mechanism. Stigmergy, in turns, enables a seamless extension to a swarm construction scenario, without the need for the introduction of explicit communication or planning strategies. The exploitation of stigmergy and templates is key to reduce the complexity of the robotic hardware and control (e.g., in terms of sensorimotor requirements, information processing, and coordination protocols), and the low precision required

for the deposition of compliant pockets supports the usage of a simple manipulation system. Overall, we believe this to be a very good demonstration of an integrated system for autonomous construction, which supports the proposal of using compliant pockets by robot swarms. In future work, it would be interesting to deploy a similar swarm construction system outdoor, exploiting a collection of UAVs capable of picking up and dropping compliant pockets quickly and reliably. This could become a viable technology in the future for quickly building levees in emergency situations.

The complexity of structures that can be built by the proposed construction system may be limited to simple barriers, possibly with varying shapes determined by the environmental template provided to the system. However, compliant pockets are not constraining in this respect [2]. To build more complex structures, we envisage the usage of an heterogeneous system in which some robots provide scaffolding to the building process. Scaffolding robots would both act as template to direct the building process toward more complex shapes, and may even support the construction of 3D roofed structures made of arcs and vaults entirely built by means of compliant pockets. More than simple scaffolding, robots could work to reduce interferences among building teammates, by limiting the number of individuals working on a particular site of the structure at the same time. By exploiting behavioral and information processing capabilities of scaffolding robots, the complexity of the built structure could be increased. In this respect, preliminary experiments using robots to provide more complex templates and interference reduction confirm the viability of the approach.

Acknowledgments

The research presented in this paper was carried out in the framework of H2SWARM, an European Science Foundation project partially funded by the Belgian F.R.S.-FNRS (contract R.70.02.11F), the Italian CNR (contract GAE_P0000412), and the Swiss NSF (grant 20BI21_134317). The work was also partially supported by the ERC Advanced Grant "E-SWARM: Engineering Swarm Intelligence Systems" (grant 246939), and by the European Union project ASCENS (n. 257414). M. Dorigo acknowledges support from the Belgian F.R.S.-FNRS.

Appendix. Parameters

The parameters used in the study are: $d_1 = 34$ cm, $d_2 = 43$ cm for the scenario; $r_c = 90$ cm, $d_m = 15$ cm for the robot; $\delta_1 = 8$ cm, $k_1 = 0.05$, $\alpha = 2$, $\delta_2 = 30$ cm, $k_2 = 1$, $\sigma = 1$ for the controller; and $h_1 = 2.3$, $h_2 = 4$ for the metrics (proportional to the pocket dimensions).

References

[1] C. Balaguer, M. Abderrahim, Robotics and Automation in Construction, InTech, 2008.
[2] G.A. Smithers, M.K. Nehls, M.A. Hovater, S.W. Evans, J.S. Miller, R.M. Broughton, D. Beale, F. Killinc-Balci, A One-Piece Lunar Regolith Bag Garage Prototype. NASA Tech. Rep., 2007.
[3] N. Khalili, Emergency Sandbag Shelter and Eco-Village: Manual-How to Build Your Own with Superadobe/Earthbags, Cal Earth Press, 2011.
[4] R. Cannon, S. Henninger, M. Levandoski, J. Perkins, J. Pitchon, R. Swats, R. Wessels, Lunar Regolith Bagging System, NASA Tech. Rep., 1990.
[5] C.A. Theriot, B. Gersey, E. Bacon, Q. Johnson, Y. Zhang, J. Norman, I. Foley, R. Wilkins, J. Zhou, H. Wu, Potential Use of In Situ Material Composites such as Regolith/Polyethylene for Shielding Space Radiation, NASA Tech. Rep., 2010.
[6] J. Werfel, K. Petersen, R. Nagpal, Designing collective behavior in a termite-inspired robot construction team, Science (6172) (2014) 754–758.
[7] G. Theraulaz, J. Gautrais, S. Camazine, J.-L. Deneubourg, The formation of spatial patterns in social insects: from simple behaviours to complex structures, Philos. Trans. R. Soc. Lond. Ser. A: Math. Phys. Eng. Sci. 361 (1807) (2003) 1263–1282.
[8] E. Bonabeau, M. Dorigo, G. Theraulaz, Swarm Intelligence, Oxford University Press, New York, 1999.
[9] M. Brambilla, E. Ferrante, M. Birattari, M. Dorigo, Swarm robotics: A review from the swarm engineering perspective, Swarm Intell. 7 (1) (2013) 1–41.
[10] M. Dorigo, M. Birattari, M. Brambilla, Swarm robotics, Scholarpedia 9 (1) (2014) 1463.
[11] T. Soleymani, V. Trianni, M. Bonani, F. Mondada, M. Dorigo, Autonomous construction with compliant building material, in: Proc. of the 13th International Conference on Intelligent Autonomous Systems (IAS), in: Advances in Intelligent Systems and Computing, vol. 302, 2014.
[12] R.A. Brooks, P. Maes, M.J. Matarić, G. More, Lunar base construction robots, in: Proc. of the 1990 IEEE International Workshop on Intelligent Robots and Systems 'Towards a New Frontier of Applications', IROS, 1990, pp. 389–392.
[13] C. Melhuish, J. Welsby, C. Edwards, Using templates for defensive wall building with autonomous mobile ant-like robots, in: Proc. of Towards Intelligent Autonomous Mobile Robots, vol. 99, 1999.
[14] J. Wawerla, G.S. Sukhatme, M.J. Matarić, Collective construction with multiple robots, in: Proc. of the 2002 IEEE/RSJ International Conference on Intelligent Robots and Systems, IROS, vol. 3, 2002, pp. 2696–2701.
[15] Q. Lindsey, D. Mellinger, V. Kumar, Construction with quadrotor teams, Auton. Robots 33 (3) (2012) 323–336.
[16] J. Willmann, F. Augugliaro, T. Cadalbert, R. D'Andrea, F. Gramazio, M. Kohler, Aerial robotic construction towards a new field of architectural research, Int. J. Archit. Comput. 10 (3) (2012) 439–460.
[17] S. Wismer, G. Hitz, M. Bonani, A. Gribovskiy, S. Magnenat, Autonomous construction of a roofed structure: Synthesizing planning and stigmergy on a mobile robot, in: Proc. of the 2012 IEEE/RSJ International Conference on Intelligent Robots and Systems, IROS, 2012, pp. 5436–5437.
[18] K. Petersen, R. Nagpal, J. Werfel, TERMES: An autonomous robotic system for three-dimensional collective construction, in: Proc. of Robotics: Science and Systems, 2011, pp. 257–264.
[19] N. Napp, R. Nagpal, Distributed amorphous ramp construction in unstructured environments, Robotica 32 (02) (2014) 279–290.
[20] S. Revzen, M. Bhoite, A. Macasieb, M. Yim, Structure synthesis on-the-fly in a modular robot, in: Proc. of the 2011 IEEE/RSJ International Conference on Intelligent Robots and Systems, IROS, 2011, pp. 4797–4802.
[21] B. Khoshnevis, M.P. Bodiford, K.H. Burks, E. Ethridge, D. Tucker, W. Kim, H. Toutanji, M.R. Fiske, Lunar contour crafting–a novel technique for ISRU-based habitat development, in: Proc. of American Institute of Aeronautics and Astronautics, AIAA, Conference, 2005, pp. 7397–7409.
[22] N. Napp, O.R. Rappoli, J.M. Wu, R. Nagpal, Materials and mechanisms for amorphous robotic construction, in: Proc. of the 2012 IEEE/RSJ International Conference on Intelligent Robots and Systems, IROS, 2012, pp. 4879–4885.
[23] M. Bonani, V. Longchamp, S. Magnenat, P. Retornaz, D. Burnier, G. Roulet, F. Vaussard, H. Bleuler, F. Mondada, The marXbot, a miniature mobile robot opening new perspectives for the collective-robotic research, in: Proc. of the 2010 IEEE/RSJ International Conference on Intelligent Robots and Systems, IROS, 2010, pp. 4187–4193.
[24] M. Dorigo, D. Floreano, L.M. Gambardella, F. Mondada, S. Nolfi, T. Baaboura, M. Birattari, M. Bonani, M. Brambilla, A. Brutschy, D. Burnier, A. Campo, A.L. Christensen, A. Decugnière, G.A. Di Caro, F. Ducatelle, E. Ferrante, A. Förster, J. Guzzi, V. Longchamp, S. Magnenat, J. Martinez Gonzales, N. Mathews, M. Montes de Oca, R. O'Grady, C. Pinciroli, G. Pini, P. Rétornaz, J. Roberts, V. Sperati, T. Stirling, A. Stranieri, T. Stützle, V. Trianni, E. Tuci, A.E. Turgut, F. Vaussard, Swarmanoid: A novel concept for the study of heterogeneous robotic swarms, IEEE Robot. Autom. Mag. 20 (4) (2013) 60–71.
[25] S. Magnenat, R. Philippsen, F. Mondada, Autonomous construction using scarce resources in unknown environments, Auton. Robots 33 (4) (2012) 467–485.
[26] T. Soleymani, V. Trianni, M. Dorigo, Calibration of omni-directional cameras based on supervised learning, Tech. rep. 2013-12, IRIDIA, Université Libre de Bruxelles, Brussels, Belgium, 2013.
[27] M.P. Wand, M.C. Jones, Kernel Smoothing, Vol. 60, CRC Press, 1994.
[28] C. Pinciroli, V. Trianni, R. O'Grady, G. Pini, A. Brutschy, M. Brambilla, N. Mathews, E. Ferrante, G.A. Di Caro, F. Ducatelle, M. Birattari, L.M. Gambardella, M. Dorigo, ARGoS: a modular, parallel, multi-engine simulator for multi-robot systems, Swarm Intell. 6 (4) (2012) 271–295.
[29] F. Ducatelle, G.A. Di Caro, C. Pinciroli, F. Mondada, L.M. Gambardella, Communication assisted navigation in robotic swarms: Self-organization and cooperation, in: Proc. of the 2011 IEEE/RSJ International Conference on Intelligent Robots and Systems, IROS, 2011, pp. 4981–4988.
[30] F. Ducatelle, G.A. Di Caro, A. Förster, M. Bonani, M. Dorigo, S. Magnenat, F. Mondada, R. O'Grady, C. Pinciroli, P. Rétornaz, V. Trianni, L.M. Gambardella, Cooperative navigation in robotic swarms, Swarm Intell. 8 (1) (2014) 1–33.
[31] G. Pini, A. Brutschy, C. Pinciroli, M. Dorigo, M. Birattari, Autonomous task partitioning in robot foraging: an approach based on cost estimation, Adapt. Behav. 21 (2) (2013) 118–136.
[32] G. Pini, A. Brutschy, M. Frison, A. Roli, M. Dorigo, M. Birattari, Task partitioning in swarms of robots: an adaptive method for strategy selection, Swarm Intell. 5 (3–4) (2011) 283–304.

Touraj Soleymani received his B.S. and M.S. degrees both on Aeronautical Engineering with emphasis on Flight Dynamics and Control from Sharif University of Technology in September 2008 and January 2011, respectively. He was a research assistant at the Artificial Intelligence Laboratory, Université Libre de Bruxelles from April 2012 to October 2014. Currently, he is a Ph.D. candidate at the Department of Electrical and Computer Engineering, Technische Universität München. His research interests include distributed control, distributed optimization, and cooperative multi-agent systems. He received the Best Paper Award of the Conference on Intelligent Autonomous Systems in 2014.

Vito Trianni is a tenured researcher at the ISTC-CNR, the Institute of Cognitive Sciences and Technologies of the Italian National Research Council. He owns a Ph.D. in Applied Sciences delivered by the Université Libre de Bruxelles in 2006. He has thorough expertise, both theoretical and experimental, in the study and design of self-organizing behaviors, especially applied to swarm robotics.

Michael Bonani works in the Mobsya Association whose aim is to promote technology via robots for education and research. Michael Bonani obtained his master and Ph.D. at the École Polytechnique Fédérale de Lausanne (EPFL). He has expertise in the mechatronic design and production of small educational robots and of collective robots. He is a co-founder of Mobsya, an association for the development of educational robots. He is author of several publications in the field of robot design.

Francesco Mondada is professor at the École Polytechnique Fédérale de Lausanne (EPFL), Switzerland. After a master and a Ph.D. received at EPFL, he led the design of many miniature mobile robots, commercialized and used worldwide in thousands of schools and universities. He cofounded several companies selling these robots or other educational tools. He is author of more than one hundred publications in the field of robot design. He received several awards, including the Swiss Latsis University prize as best young researcher at EPFL, and the Credit Suisse Award for Best Teaching as best teacher at EPFL.

Marco Dorigo received the Laurea, Master of Technology, degree in industrial technologies engineering in 1986, and the Ph.D. degree in electronic engineering in 1992 from the Politecnico di Milano, Milan, Italy, and the title of Agrégé de l'Enseignement Supérieur, from ULB, in 1995. From 1992 to 1993, he was a Research Fellow at the International Computer Science Institute, Berkeley, CA. In 1993, he was a NATO-CNR Fellow, and from 1994 to 1996, a Marie Curie Fellow. Since 1996, he has been a tenured Researcher of the FNRS, the Belgian National Funds for Scientific Research, and co-director of IRIDIA, the artificial intelligence laboratory of the ULB. He is the inventor of the ant colony optimization metaheuristic. His current research interests include swarm intelligence, swarm robotics, and metaheuristics for discrete optimization. He is the Editor-in-Chief of Swarm Intelligence, and an Associate Editor or member of the Editorial Boards of many journals on computational intelligence and adaptive systems. Dr. Dorigo is a Fellow of IEEE, AAAI, and ECCAI. He was awarded the Italian Prize for Artificial Intelligence in 1996, the Marie Curie Excellence Award in 2003, the Dr. A. De Leeuw-Damry-Bourlart award in applied sciences in 2005, the Cajastur International Prize for Soft Computing in 2007, an ERC Advanced Grant in 2010, and the IEEE Frank Rosenblatt Award in 2015.